DIGITAL CONTROLLERS FOR VTOL AIRCRAFT*

Robert F. Stengel, John R. Broussard, and Paul W. Berry

THE ANALYTIC SCIENCES CORPORATION
Six Jacob Way
Reading, Massachusetts 01867

ABSTRACT

Using linear-optimal estimation and control techniques, digital-adaptive control laws have been designed for a tandem-rotor helicopter which is equipped for fully automatic flight in terminal area operations. Two distinct discrete-time control laws are designed to interface with velocity-command and attitude-command guidance logic, and each incorporates proportional-integral compensation for non-zero-set-point regulation, as well as reduced-order Kalman filters for sensor blending and noise rejection. Adaptation to flight condition is achieved with a novel gain-scheduling method based on correlation and regression analysis. The linear-optimal design approach is found to be a valuable tool in the development of practical multivariable control laws for vehicles which evidence significant coupling and insufficient natural stability.

1. INTRODUCTION

Vertical Takeoff and Landing (VTOL) aircraft are able to operate from small landing areas and in the vicinity of obstacles which would prevent the operation of conventional aircraft. To conduct scheduled operations in adverse weather with these aircraft, whose unaugmented flying qualities may be marginal, automatic control is required. The VTOL Approach and Landing Technology (VALT) Program of the National Aeronautics and Space Administration is developing a technology base in navigation, guidance, control, display, and flight management requirments for future VTOL aircraft. This paper describes digital control system design procedures being developed under this program, as well as preliminary control structures (Ref. 1) for the VALT Research Aircraft -- a tandem-rotor, medium transport helicopter (Fig. 1).

Significant features of the VTOL digital control design process which are discussed include the design of discrete-time proportional-integral controllers to meet continuous-time specifications, discrete-

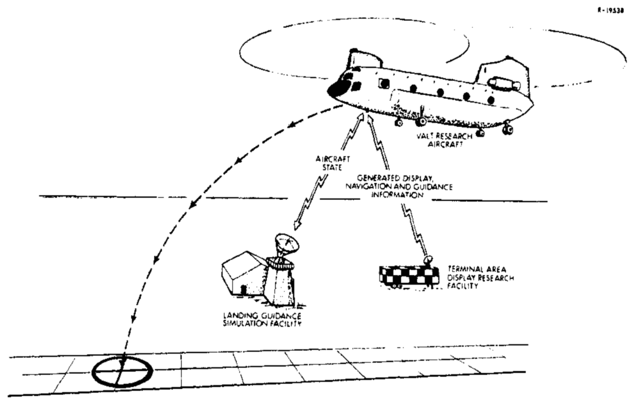

Figure 1 VALT Research Facilities

time estimation of continuous-time systems, adaptation to varying flight conditions, and evaluation of control system response. The resulting linear-optimal control laws correspond to "classical" control laws in their use of proportional-integral compensation, gain scheduling, and linear feedback/crossfeed loops. The optimal laws are designed with considerably less effort and reliance on the designer's intuition than equivalent classical control laws. They can operate at lower sampling rates, and they achieve equivalent or superior performance in command response and disturbance rejection.

2. VEHICLE AND CONTROL SYSTEM CHARACTERISTICS

While the control design techniques presented in this paper could be applied to a wide variety of aircraft types, the particular configuration under consideration is a tandem-rotor helicopter (Fig. 1). The strong pitching moment afforded by separate rotors permits large variation of the center of gravity, and the two rotors provide a large load-carrying capacity; however, the thrust interference of the rotors can degrade stability and flying qualities of the unaugmented airframe (Refs. 2 and 3). In forward flight, the short period and Dutch roll modes of motion may be statically unstable, and roll damping is likely to be low. Speed stability can be negative during cruise and too

*This work was conducted under Contracts No. NAS1-13807 and NAS1-14358 for the NASA Langley Research Center.

positive at hover. It generally proves desirable to provide an automatic stability augmentation system (SAS) for the tandem-rotor helicopter, and the production version of the VALT Research Aircraft obtains substantial flying qualities improvements from a dual-redundant SAS.

The VALT Research Aircraft typically carries payloads of up to 4000 kg (8800 lb), and its normal operating weight is 15,000 kg (33,000 lb). It operates at indicated airspeeds below 80 m/s (160 kt) and altitudes up to 4250 m (14,000 ft). There are 4 primary control variables resulting from gang and differential commands to the collective and cyclic deflections of the two rotors. These provide control moments about all three axes, as well as vertical force; horizontal forces are obtained by tilting the entire vehicle to provide a component of rotor lift in the desired direction. Control linkages and actuators resolve commands issued by the pilot or VALT Navigation, Guidance, and Control (NGC) System into the appropriate rotor deflections, as shown in Fig. 2.

R-19353

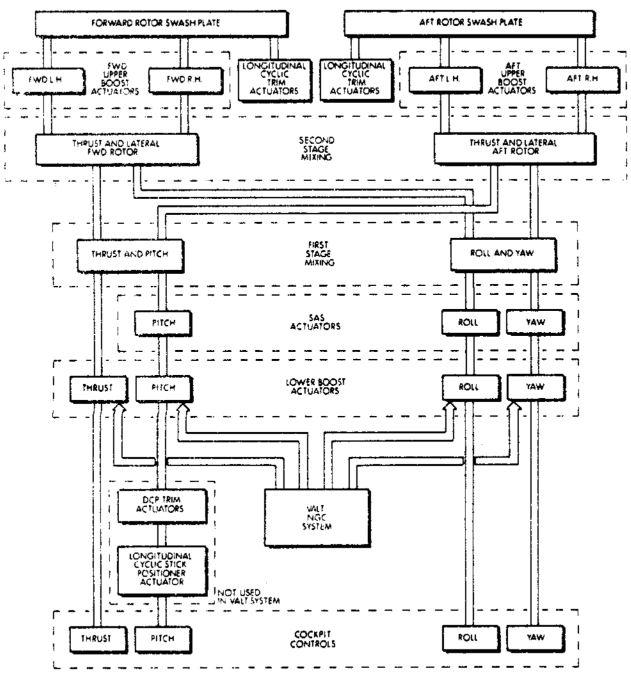

Figure 2 Control Mechanization in the VALT Research Aircraft

The VALT NGC System is, itself, a research tool; hence, its configuration is subject to change. For purposes of control system design, the NGC System is assumed to contain rate gyros, linear accelerometers, vertical and heading gyros, barometric altimeter, airspeed indicator, digital computer, and appropriate interfaces. The system obtains navigation information from an external terminal area aid, e.g., a microwave landing system.

3. CONTROL OBJECTIVES AND RESPONSE CRITERIA

In defining control objectives, the first area of concern is how to distinguish between "guidance" and "control" functions, for each is a regulating mechanism which is required to keep a vehicle on its intended path. Guidance is associated with the translational motions of the vehicle in an earth-relative frame; hence, the guidance logic accepts position inputs and issues velocity or acceleration commands. As indicated in the previous section, helicopters generate horizontal forces by tilting the primary lift vector, so horizontal acceleration commands can be transformed readily to attitude commands. Control is more closely allied with angular motions and dynamic stability of the aircraft; therefore, the control logic accepts guidance inputs and issues commands to the control effectors. In most cases, the guidance and control feedback paths are approximately concentric, i.e., they possess an outer/inner-loop structure which allows the major portions of guidance and control design to be conducted separately. Only the control functions are treated in this paper; guidance functions are discussed in Refs., 1, 4, and 5.

Neglecting disturbance inputs, the nonlinear equations which govern vehicle motion can be written as the vector differential equation

$$\dot{\underline{x}}(t) = \underline{f}[\underline{x}(t), \underline{u}(t)] \qquad (1)$$

For the rigid-body control problem, the state vector contains 3 components each of translational rate, angular rate, and attitude,

$$\underline{x}^T = [\, u \;\; v \;\; w \;\; p \;\; q \;\; r \;\; \theta \;\; \phi \;\; \psi \,] \qquad (2)$$

where (u,v,w) are body-axis velocities, (p,q,r) are body-axis rotational rates, and (θ,ϕ,ψ) are Euler angles of the body axes with respect to an Earth-relative frame. The control vector includes differential collective, gang collective, gang cyclic, and differential cyclic rotor deflections:

$$\underline{u}^T = [\, \delta_B \;\; \delta_C \;\; \delta_S \;\; \delta_R \,] \qquad (3)$$

The total state and control can be divided into nominal and perturbation components,

$$\underline{x}(t) = \underline{x}_o(t) + \Delta\underline{x}(t) \qquad (4)$$

$$\underline{u}(t) = \underline{u}_o(t) + \Delta\underline{u}(t) \qquad (5)$$

leading to a first-order Taylor series expansion of Eq. (1):

$$\dot{\underline{x}}_o(t) = \underline{f}[\underline{x}_o(t), \underline{u}_o(t)] \qquad (6)$$

$$\Delta \dot{\underline{x}}(t) = F(t)\, \Delta \underline{x}(t) + G(t)\, \Delta \underline{u}(t) \quad (7)$$

where

$$F(t) = \frac{\partial}{\partial \underline{x}} \underline{f}\, [\underline{x}_o(t),\, \underline{u}_o(t)] \quad (8)$$

$$G(t) = \frac{\partial}{\partial \underline{u}} \underline{f}\, [\underline{x}_o(t),\, \underline{u}_o(t)] \quad (9)$$

In principle, $\underline{x}_o(t)$, $\underline{u}_o(t)$, F(t), and G(t) must be found for every possible flight profile; however, certain observations and assumptions can be involved in designing control logic which provides $\underline{u}(t)$. The nominal control, $\underline{u}_o(t)$, serves as a dynamic control trim setting in Eq. 5. It need not provide exact open-loop control -- in fact, the closed-loop logic which provides $\Delta\underline{u}(t)$ should adjust to follow the desired path even if $\underline{u}_o(t)$ is incorrect, as variations in trim settings due to weight, center-of-gravity location, and aircraft-to-aircraft variations can be expected. This suggests that the closed-loop control laws should contain integrating action to null steady-state errors. (Further discussion of $\underline{u}_o$ computation can be found in Ref. 1). F(t) and G(t) are slowly varying functions of time -- actually, they are explicit functions of the flight condition rather than time; hence, control laws can be formed at specific points in the flight envelope and need not be referenced to specific flight profiles. This leads to control laws based on linear-time-invariant models of aircraft motion which are adapted to changing flight conditions by gain scheduling, i.e., by storing control gains as functions of flight variables.

Since attitude-command and velocity-command guidance laws are both candidates for implementation on future VTOL aircraft, associated control laws must be designed. In both cases, the control logic must provide trim and command the appropriate control actuators; however, the control law inputs, $\underline{y}_d$, differ. For the attitude-command control law, 3 Euler angles and vertical velocity are commanded:

$$\underline{y}_d^T = [\ \theta_d\ \phi_d\ \psi_d\ V_{z_d}\ ] \quad (10)$$

For the velocity-command control law, yaw angle and the translational velocity components expressed in an earth-relative frame are commanded:

$$\underline{y}_d^T = [\ V_{x_d}\ V_{y_d}\ V_{z_d}\ \psi_d\ ] \quad (11)$$

Step response criteria are specified for both control laws using conventional figures of merit: rise time, overshoot, and settling time. For example, the aircraft's response to horizontal velocity commands must reach 80% of the final value within 4 sec, with overshoots no greater than 4 to 20% (depending on forward speed). Angle response of the attitude-command control law must achieve 90% of the final value within 1.5 sec, with no more than 15% overshoot, and with a ±5% settling time of 5 sec or less. Vertical velocity step response using either law must reach 90% of the final value in 2 sec with overshoots below 5 to 20%.

The quadratic synthesis technique of designing control systems (described below) is not formulated in terms of step response criteria; the design parameters are coefficients which weight the mean-square variations in state and control. Nevertheless, it is found that these weighting coefficients provide flexible and efficient means of adjusting close-loop response to meet step response requirements. Furthermore, the control laws developed in the next section have gains which are designed explicitly to keep control actuator rates and displacements within acceptable limits for normal command and disturbance inputs.

4. CONTROL LAW DEVELOPMENT*

The attitude-command and velocity-command control laws have many similarities, but their structures are fundamentally different. Both are sampled-data linear-optimal servos, in that they use discrete-time logic to control a continuous-time system, and both contain separate elements for estimation and control. The state estimator is the same in both cases; however, the proportional-integral structures chosen for the two laws demonstrate distinct alternatives for "Type 1" control.† The attitude-command control law contains a proportional-integral (PI) structure which provides zero steady-state step response error using integrating action and control-rate restraint through the use of modest gain magnitudes. The velocity-command control law contains a proportional-integral-filter (PIF) structure which provides Type-1 response and which restricts control rates with a bank of low-pass filters on the command outputs.

Each of the discrete-time control structures is rigorously obtained by augmenting the system state equation (Eq. 7), defining a continuous-time quadratic cost function, J, and transforming the state equation and the cost function to their discrete-time equivalents, as in

*The participation of M. Safonov and M. Athans in the development of controller structures is acknowledged.

†A Type 1 System contains one pure integration in series with each control actuator; hence, it can achieve zero steady-state error in resonse to a step input, if properly designed (Ref. 6).

Ref. 7. The PI and PIF structures result from differing state augmentation and cost function definitions, as described below.

Attitude-Command (PI) Control Structure

A derivation for the discrete-time PI control structure is summarized in this section; additional details can be found in Ref. 1 and in future documentation of the VALT control design program. The state vector is augmented to contain not only the aircraft's motion variables but its control variables, and this new system is driven by control rate inputs, $\Delta \underline{v}(t)$. This leads to the continuous-time state equation,

$$\begin{bmatrix} \Delta\dot{\underline{x}}(t) \\ \Delta\dot{\underline{u}}(t) \end{bmatrix} = \begin{bmatrix} F & G \\ 0 & 0 \end{bmatrix} \begin{bmatrix} \Delta\underline{x}(t) \\ \Delta\underline{u}(t) \end{bmatrix} + \begin{bmatrix} 0 \\ I \end{bmatrix} \Delta\underline{v}(t) \tag{12}$$

The discrete-time equivalent, which propagates the state from the k^{th} to $(k+1)^{st}$ sampling instant, is

$$\begin{bmatrix} \Delta\underline{x} \\ \Delta\underline{u} \end{bmatrix}_{k+1} = \begin{bmatrix} \Phi & \Gamma \\ 0 & I \end{bmatrix} \begin{bmatrix} \Delta\underline{x} \\ \Delta\underline{u} \end{bmatrix}_k + \begin{bmatrix} (\sim 0) \\ \Delta t I \end{bmatrix} \Delta\underline{v}_k$$

$$= \bar{\Phi} \begin{bmatrix} \Delta\underline{x} \\ \Delta\underline{u} \end{bmatrix}_k + \bar{\Gamma}\, \Delta\underline{v}_k \tag{13}$$

In these equations, F and G are assumed time-invariant, Φ and Γ are the corresponding state-transition and discrete control-effect matrices (for sampling interval, Δt), and I is a (4x4) identity matrix. The control difference vector, $\Delta\underline{v}_k = (\Delta\underline{u}_{k+1} - \Delta\underline{u}_k)/\Delta t$, is the discrete-time equivalent of $\Delta\underline{v}(t)$; it has a direct effect on the propagation of both $\Delta\underline{x}_{k+1}$ and $\Delta\underline{u}_{k+1}$; however, its effect on $\Delta\underline{x}_{k+1}$ is $O(\Delta t^2)$ and is assumed negligible.

The continuous-time quadratic cost function to be minimized by control is

$$J = \int_0^\infty \left\{ [\Delta\underline{x}^T(t) \Delta\underline{u}^T(t)]\, Q \begin{bmatrix} \Delta\underline{x}(t) \\ \Delta\underline{u}(t) \end{bmatrix} + \Delta\underline{v}^T(t)\, R\, \Delta\underline{v}(t) \right\} dt \tag{14}$$

where Q and R are matrices which weight state, control, and control rate perturbations. The elements of Q and R are the major design parameters for designing the discrete-time PI controller. As shown in Ref. 7, Q and R (together with F, G, and Δt) define weighting matrices ($\hat{Q}, \hat{M}, \hat{R}$) in a discrete-time expression of Eq. 14 which contains cross-product weighting of the state and control (Eq. 22 below).

The Type-1 property is associated with steady-state response to a command input (or non-zero set point) imposed at k=0, which may be a transformation of motion variables:

$$\Delta\underline{y}_d = T \Delta\underline{x}_d \tag{15}$$

(In the present case, Eq. 10 indicates that the transformation matrix, T, is a (9x4) matrix containing null and identity subsets as well as a body-to-earth-axis transformation for vertical velocity.) If an equilibrium solution exists, the motion and control variables take on constant values, $\Delta\underline{x}^*$ and $\Delta\underline{u}^*$, and the following equation is satisfied (with I having proper dimension):

$$\begin{bmatrix} 0 \\ \Delta\underline{y}_d \end{bmatrix} = \begin{bmatrix} (\Phi - I) & \Gamma \\ T & 0 \end{bmatrix} \begin{bmatrix} \Delta\underline{x}^* \\ \Delta\underline{u}^* \end{bmatrix} \tag{16}$$

To assure that $\Delta\underline{x}^*$ and $\Delta\underline{u}^*$ exist and are unique for every choice of $\Delta\underline{y}_d$, the composite matrix must possess an inverse:

$$\begin{bmatrix} (\Phi - I) & \Gamma \\ T & 0 \end{bmatrix}^{-1} \equiv \begin{bmatrix} S_{11} & S_{12} \\ S_{21} & S_{22} \end{bmatrix} \tag{17}$$

Then

$$\Delta\underline{x}^* = S_{12}\Delta\underline{y}_d \; ; \; \Delta\underline{u}^* = S_{22}\Delta\underline{y}_d \tag{18,19}$$

and the perturbation variables can be redefined with respect to their non-zero set points:

$$\Delta\tilde{\underline{x}} = \Delta\underline{x} - \Delta\underline{x}^* \; ; \; \Delta\tilde{\underline{u}} = \Delta\underline{u} - \Delta\underline{u}^* \tag{20,21}$$

($\Delta\tilde{\underline{v}} = \Delta\underline{v}$, since the steady-state control difference is zero.) The discrete-time equivalent of Eq. 14 now can be written as the "cost" of deviating from the non-zero set point:

$$J = \sum_{k=-1}^{\infty} \left\{ \left[\Delta\tilde{\underline{x}}^T \Delta\tilde{\underline{u}}^T\right]_k \hat{Q} \begin{bmatrix} \Delta\tilde{\underline{x}} \\ \Delta\tilde{\underline{u}} \end{bmatrix}_k + \left[\Delta\tilde{\underline{x}}^T \; \Delta\tilde{\underline{u}}^T\right]_k \hat{M}\, \Delta\tilde{\underline{v}}_k + \Delta\tilde{\underline{v}}^T{}_k\, \hat{R}\, \Delta\tilde{\underline{v}}_k \right\} \tag{22}$$

Note that the summation necessarily begins at the -1^{st} sampling instant because the control difference for a step occuring at k = 0 depends on the value of the control at k=-1. This initial difference is likely to have larger magnitude than any succeeding difference; therefore, it is essential that the discrete-time cost function for the sampled-data servo be written as in Eq. 22.

The control law which minimizes Eq. 22 specifies the control difference as a linear function of motion and control variables,

$$\Delta\tilde{\underline{v}}_k = -(\hat{R} + \bar{\Gamma}^T P \bar{\Gamma})^{-1}(\bar{\Gamma}^T P\,\bar{\Phi} + \hat{M}^T)\begin{bmatrix}\Delta\tilde{\underline{x}}\\ \Delta\tilde{\underline{u}}\end{bmatrix}_k$$

$$= -K_1\Delta\tilde{\underline{x}}_k - K_2\Delta\tilde{\underline{u}}_k \qquad (23)$$

where P is the steady-state solution of a discrete-time Riccati equation:

$$P = \bar{\Phi}^T P \bar{\Phi} + \hat{Q}$$

$$-\ (\bar{\Gamma}^T P\bar{\Phi} + \hat{M}^T)^T(\hat{R} + \bar{\Gamma}^T P \bar{\Gamma})^{-1}(\bar{\Gamma}^T P \bar{\Phi} + \hat{M}^T) \qquad (24)$$

Control position (rather than difference) is the required output, so Eq. 23 is rewritten as

$$\Delta\tilde{\underline{u}}_k = \Delta\tilde{\underline{u}}_{k-1} - \Delta t K_1 \Delta\tilde{\underline{x}}_{k-1} - \Delta t K_2 \Delta\tilde{\underline{u}}_{k-1}$$

$$= -\Delta t K_1 \Delta\tilde{\underline{x}}_{k-1} + (I - \Delta t K_2)\Delta\tilde{\underline{u}}_{k-1} \qquad (25)$$

This control law does not have the Type-1 property, because the term $\Delta t K_2$ destroys the pure numerical integrating feature which can be obtained by accumulating the past control; however, knowledge of system dynamics can be used to introduce the Type-1 property. Equation 17 is used to define the transformed gain matrices, C_1 and C_2:

$$\begin{bmatrix} C_1 & C_2 \end{bmatrix}\begin{bmatrix} (\Phi - I) & \Gamma \\ T & 0 \end{bmatrix} = \begin{bmatrix} \Delta t K_1 & \Delta t K_2 \end{bmatrix} \qquad (26)$$

or

$$C_1 = \Delta t K_1 S_{11} + \Delta t K_2 S_{21} \qquad (27)$$

$$C_2 = \Delta t K_1 S_{12} + \Delta t K_2 S_{22} \qquad (28)$$

Equation 25 then can be written as

$$\Delta\tilde{\underline{u}}_k = \Delta\tilde{\underline{u}}_{k-1} - C_1(\Delta\tilde{\underline{x}}_k - \Delta\tilde{\underline{x}}_{k-1})$$

$$-\ C_2 T \Delta\tilde{\underline{x}}_{k-1} \qquad (29)$$

Reverting to the original definitions of perturbation variables, the PI control law is

$$\Delta\underline{u}_k = \Delta\underline{u}_{k-1} - C_1(\Delta\underline{x}_k - \Delta\underline{x}_{k-1}) +$$

$$C_2(\Delta\underline{y}_{d_k} - T\Delta\underline{x}_{k-1}) \qquad (30)$$

Use of the term, $\Delta\underline{y}_{d_k}$ (rather than $\Delta\underline{y}_{d_{k-1}}$), is consistent with the definition of the non-zero set point; at k=0, the set point is defined by $\Delta\underline{y}_{d_0}$, not $\Delta\underline{y}_{d_{-1}}$. Equation 30 has the necessary integrating action for Type-1 control as $k\to\infty$ (and assuming an asymptotically stable closed-loop system and no change in $\Delta\underline{y}_d$); the driving terms vanish, and $\Delta\underline{u}_k \to \Delta\underline{u}_{k-1}$. A block diagram of the PI controller is illustrated by Fig. 3.

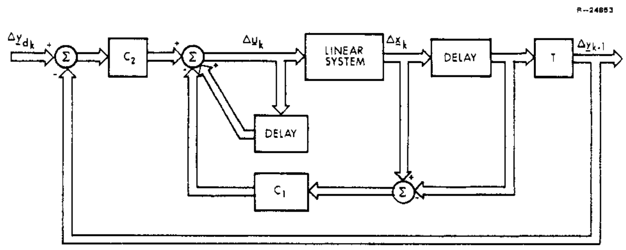

Figure 3 Structure of the Attitude-Command Proportional-Integral (PI) Controller

Velocity-Command (PIF) Control Structure

The derivation of the discrete-time PIF control structure is similar to the PI derivation; hence, the principal differences are summarized here. The augmented discrete-time dynamic equation (Eq. 13) is augmented once again, with explicit "integrator states", $\Delta\underline{\xi}$, which operate on the error between $\Delta\underline{y}_d$ and $T\Delta\underline{x}$:

$$\begin{bmatrix}\Delta\underline{x}\\ \Delta\underline{u}\\ \Delta\underline{\xi}\end{bmatrix}_{k+1} = \begin{bmatrix}\Phi & \Gamma & 0\\ 0 & I & 0\\ \Delta t T & 0 & I\end{bmatrix}\begin{bmatrix}\Delta\underline{x}\\ \Delta\underline{u}\\ \Delta\underline{\xi}\end{bmatrix}_k$$

$$+ \begin{bmatrix}0\\ \Delta t I\\ 0\end{bmatrix}\Delta\underline{v}_k - \begin{bmatrix}0\\ 0\\ \Delta t I\end{bmatrix}\Delta\underline{y}_{d_{k+1}} \qquad (31)$$

The transformation matrix, T, for the velocity-command controller contains a body-to-earth-axis coordinate change for velocity components, as indicated by Eq. 11, as well as null and identity subsets.

The perturbation variables are redefined with respect to their non-zero set points. $\Delta\tilde{\underline{x}}$ and $\Delta\tilde{\underline{u}}$, are defined as before, and,

$\Delta\tilde{\underline{\xi}} = \Delta\underline{\xi} - \Delta\underline{\xi}^*$, where $\Delta\underline{\xi}^*$ is the steady-state value to be specified. With the perturbation shift, the last term in Eq. 31 vanishes, and the equation can be written in the form

$$\begin{bmatrix} \Delta\tilde{\underline{x}} \\ \Delta\tilde{\underline{u}} \\ \Delta\tilde{\underline{\xi}} \end{bmatrix}_{k+1} = \bar{\Phi} \begin{bmatrix} \Delta\tilde{\underline{x}} \\ \Delta\tilde{\underline{u}} \\ \Delta\tilde{\underline{\xi}} \end{bmatrix}_k + \bar{\Gamma}\, \Delta\tilde{\underline{v}}_k \qquad (32)$$

The discrete-time cost function to be minimized by control is

$$J = \sum_{k=-1}^{\infty} \left\{ \begin{bmatrix} \Delta\tilde{\underline{x}}^T \Delta\tilde{\underline{u}}^T \Delta\tilde{\underline{\xi}}^T \end{bmatrix}_k \hat{Q} \begin{bmatrix} \Delta\tilde{\underline{x}} \\ \Delta\tilde{\underline{u}} \\ \Delta\tilde{\underline{\xi}} \end{bmatrix}_k + \begin{bmatrix} \Delta\tilde{\underline{x}}^T \Delta\tilde{\underline{u}}^T \Delta\tilde{\underline{\xi}}^T \end{bmatrix}_k \hat{M} \begin{bmatrix} \Delta\tilde{\underline{x}} \\ \Delta\tilde{\underline{u}} \\ \Delta\tilde{\underline{\xi}} \end{bmatrix}_k + \Delta\tilde{\underline{v}}_k^T \hat{R} \Delta\tilde{\underline{v}}_k \right\} \qquad (33)$$

The control law which minimizes Eq.33 is

$$\Delta\tilde{\underline{v}}_k = -(\hat{R} + \bar{\Gamma}^T P \bar{\Gamma})^{-1} (\bar{\Gamma}^T P \bar{\Phi} + \hat{M}^T) \begin{bmatrix} \Delta\tilde{\underline{x}} \\ \Delta\tilde{\underline{u}} \\ \Delta\tilde{\underline{\xi}} \end{bmatrix}_k$$

$$= -K_1 \Delta\tilde{\underline{x}}_k - K_2 \Delta\tilde{\underline{u}}_k - K_3 \Delta\tilde{\underline{\xi}}_k \qquad (34)$$

where P is computed by Eq. 24, and all matrices ($\bar{\Phi}, \bar{\Gamma}, \hat{Q}, \hat{M}$, and $\hat{R}$) are appropriately defined and dimensioned for the augmented dynamic system (Eq. 31). This control law is manipulated to provide a control position command, and the integrator states must be propagated to form a complete controller.

Before writing the PIF controller in terms of the original perturbation variables, it is useful to determine the proper value of $\Delta\underline{\xi}^*$, which was not specified by Eq. 16. A reasonable choice of $\Delta\underline{\xi}^*$ is that which minimizes the cost function (Eq. 33). The minimum value of J which results from closed-loop control is

$$J_{min} = \begin{bmatrix} \Delta\tilde{\underline{x}}^T \Delta\tilde{\underline{u}}^T \Delta\tilde{\underline{\xi}}^T \end{bmatrix}_{-1} P \begin{bmatrix} \Delta\tilde{\underline{x}} \\ \Delta\tilde{\underline{u}} \\ \Delta\tilde{\underline{\xi}} \end{bmatrix}_{-1} \qquad (35)$$

and the minimizing value of $\Delta\underline{\xi}^*$ is found by evaluating

$$\frac{\partial J_{min}}{\partial \Delta\tilde{\underline{\xi}}_{-1}} = 0 \qquad (36)$$

This leads to

$$\Delta\underline{\xi}^* = -P_{\xi\xi}^{-1}(P_{x\xi}^T S_{12} + P_{u\xi}^T S_{22})\Delta\underline{y}_d \qquad (37)$$

where $P_{\xi\xi}$, $P_{x\xi}$, and $P_{u\xi}$ are the appropriate partitions of P, and S_{12} and S_{22} are definded by Eq. 17. Then the PIF controller is defined by the 2 equations.

$$\Delta\underline{u}_k = (I-C_2)\Delta\underline{u}_{k-1} - C_1\Delta\underline{x}_{k-1} - C_3\Delta\underline{\xi}_{k-1} + C_4\Delta\underline{y}_{d_k} \qquad (38)$$

$$\Delta\underline{\xi}_k = \Delta\underline{\xi}_{k-1} + \Delta t(T\Delta\underline{x}_{k-1} - \Delta\underline{y}_{d_k}) \qquad (39)$$

where

$$(C_1\ C_2\ C_3) = \Delta t(K_1\ K_2\ K_3) \qquad (40)$$

$$C_4 = \Delta t\left[K_1 S_{12} + K_2 S_{22} - K_3 P_{\xi\xi}^{-1}(P_{x\xi}^T S_{12} + P_{u\xi}^T S_{22})\right] \qquad (41)$$

The PIF controller obtains low-pass filtering from $(I-C_2)\Delta\underline{u}_{k-1}$ in Eq. 38 and integrating action from Eq. 39, resulting in a Type-1 controller with control-rate restraint. The PIF structure is diagrammed in Fig. 4.

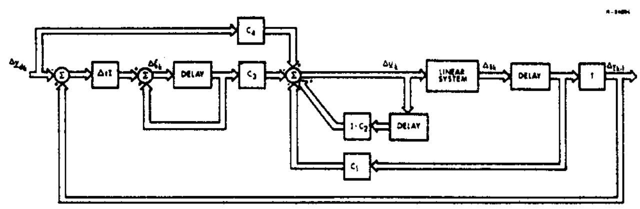

Figure 4 Structure of the Velocity-Command Proportional-Integral-Filter (PIF) Controller

Estimator Structure

Both controllers require full-state feedback to achieve the desired command response. Although the VALT instrumentation measures all these states (Eq. 2), the measurements cannot be used without filtering (to reduce errors) and, for certain components, coordinate transformation. It is necessary to design digital filters which perform these functions in a practical manner.

The optimal estimator for a physical system described by Eq. 7 is a full-state Kalman filter (Ref. 8); however, such a filter is overly complex for this application. If all states are measured, and if the measurement noise is less than the "process noise" (consisting of random inputs and system uncertainties), the Kalman filter effectively decouples into a bank of reduced-order Kalman filters. Furthermore, these filters are found to be analogous to low-pass and complementary filters, both of which are used extensively in conventional aircraft control systems. All of the filters have the general form

$$\Delta\hat{\underline{x}}_k = \Phi\ \Delta\hat{\underline{x}}_{k-1} + L\left[\Delta\underline{z}_k - H\ \Phi\ \Delta\hat{\underline{x}}_{k-1}\right] \quad (42)$$

which incorporates measurements, $\Delta\underline{z}$, in the state estimate, $\Delta\hat{\underline{x}}$. For the reduced-order filters, the state-transition matrix, Φ, defines simplified mathematical models (e.g., random walk and Markov processes), the gain matrix, L, is a function of signal and noise levels, and H transforms state components to measurement coordinates.

The 3 angular rate filters model each measurement process as a random walk with an input from a body-mounted rate gyro. The scalar roll-rate filter is

$$\hat{p}_k = \hat{p}_{k-1} + L_p(p_{m_k} - \hat{p}_{k-1}) \quad (43)$$

and the pitch-rate and yaw-rate filters are similarly defined. The 3 body-axis rates are used directly and are transformed to Euler angle rates ($\hat{\dot{\phi}}_k$, $\hat{\dot{\theta}}_k$, and $\hat{\dot{\psi}}_k$) for incorporation in the attitude filters, which model each measurement process as a random walk. The filters use Euler angle rate estimates and vertical/heading gyro inputs. For example, the roll-attitude filter is

$$\hat{\phi}_k = \hat{\phi}_{k-1} + L_{\dot{\phi}}\hat{\dot{\phi}}_{k-1} + cL_\phi(\phi_{m_k} - \hat{\phi}_{k-1})\ ,\ 0<c<1 \quad (44)$$

The gains, $L_{\dot{\phi}}$ and L_ϕ, are constant; however, c attenuates the vertical gyro residual gain in steep bank angles to minimize errors due to centrifugal forces on the gyro's erection mechanism.

The translational velocity filters are higher order, in that they must combine data from dissimilar sensors and correct for accelerometer bias and position errors. They are derived from Eq. 42 and take the form of complementary filters.

Control Law Adaptation

A comprehensive gain scheduling procedure was chosen for control law adaptation. Unlike implicit-adaptive techniques, system gains adapt to flight condition without forcing by gusts or control inputs. On-board computations for gain adaptation are minimal, adaptation time is rapid, and the structure of the linear-optimal controller is maintained.

There are 3 steps in the development of gain schedules: determination of means and standard deviations of all gains (summed over all design flight conditions), determination of correlation coefficients between gains and flight conditions, and curve fitting of gains to flight conditions by regression analysis. Further details can be found in Ref. 1.

5. EXAMPLES OF SYSTEM RESPONSE

Step response criteria have been met with both control structures at 19 flight conditions representing hover, forward flight, climb, dive, and rearward flight using sampling rates of 12 per sec. These excellent response characteristics require gains to vary with flight condition. Some adjustment of state weighting (Q) is required during the design process; however, once a satisfactory set of weights is found for a single working point, it is relatively easy to adjust weights for the remaining working points (Ref. 1).

Figures 5 and 6 illustrate attitude-command response in hover and in descending forward flight, respectively. Roll angle response is essentially unchanged with flight condition, while V_Z and θ response are shown to be well-damped and within specification.

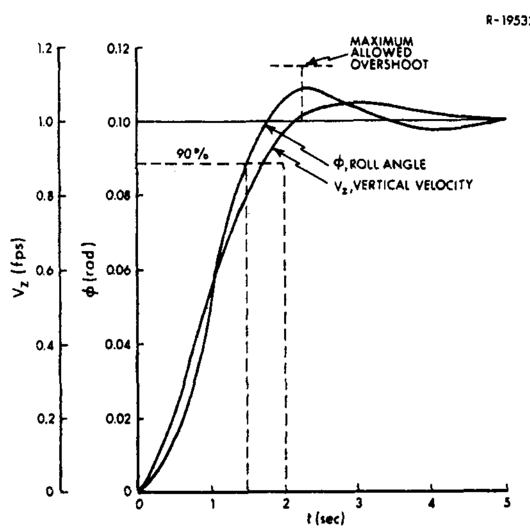

Figure 5 Attitude-Command Response in Hover

Similarly, the velocity-command response is satisfactory at both flight conditions (Figs. 7 and 8). There is little change

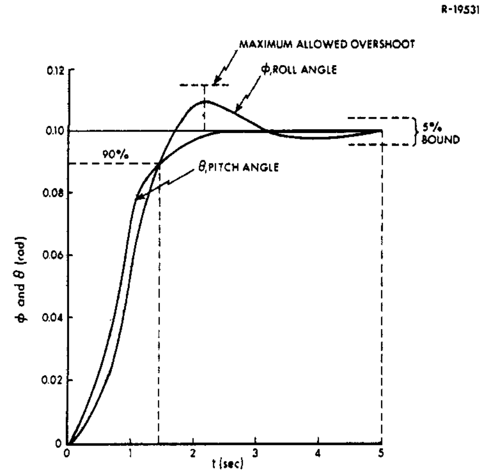

Figure 6 Attitude-Command Response in Forward, Descending Flight (V_x=120 kt, V_z=2000 fpm)

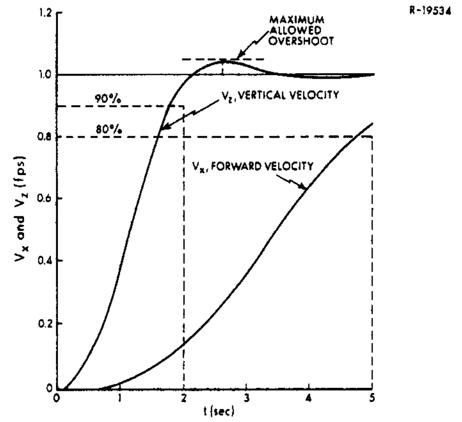

Figure 7 Velocity-Command Response in Hover

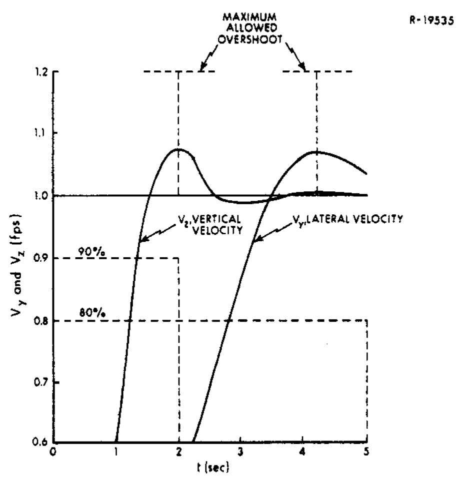

Figure 8 Velocity-Command Response in Forward, Descending Flight (V_x= 120 kt, V_z = 2000 fpm).

in V_z response, V_x is within rise-time limits at hover, and V_y response is rapid during forward flight.

6. CONCLUSIONS

The PI and PIF control structures which are presented here provide precise and efficient command response for VTOL aircraft, and they are suitable for digital control of a wide variety of other dynamic processes. A principal advantage of this design approach is that the necessary control structure is visible at an early stage of the design process. All reasonable state-control paths are identified, allowing the designer to evaluate the relative importance of each control path and to eliminate those which contribute little to system response. Adaptation, noise rejection, and non-zero set point control with digital computers can be achieved readily using the techniques of linear-optimal control.

REFERENCES

1. Stengel, R.F., Broussard, J.R., and Berry, P.W., "The Design of Digital-Adaptive Controllers for VTOL Aircraft," NASA CR-144912, March 1976.

2. Seckel, E., Stability and Control of Airplanes and Helicopters, Academic Press, New York, 1964.

3. Anon., "Fundamentals of Helicopter Stability and Control," Boeing Vertol Report No. R242, February 1961.

4. Hoffman, W.C., Zvara, J., Bryson, A.E., Jr., and Ham, N.D., "An Automatic Guidance Concept for VTOL Aircraft, AIAA Paper No. 70-1035, New York, Aug. 1970.

5. Hoffman, W.C. and Hollister, W.M., "A Spiral Guidance Approach Concept for Commercial VTOL Operations," NASA CR-132651, May 1975.

6. Sandell, N., Jr. and Athans, M., "On Type-L Multivariable Linear Systems," Automatica, Vol. 9, No. 1, Jan. 1973, pp. 131-136.

7. Dorato, P. and Levis, A.H., "Optimal Linear Regulators: The Discrete-Time Case," IEEE Trans. Auto Control, Vol. AC-16, No.6, Dec. 1971, pp. 613-620.

8. Athans, M., "The Role and Use of the Stochastic Linear-Quadratic-Gaussian Problem in Control System Design," IEEE Trans. Auto Control, Vol. AC-16, No. 6, December 1971, pp. 529-552.